



ELSEVIER

17 May 1999

PHYSICS LETTERS A

Physics Letters A 255 (1999) 287–293

Chaotic direction-reversing waves

Edgar Knobloch^{a,1}, Adam S. Landsberg^b, Jeff Moehlis^a^a Department of Physics, University of California, Berkeley, CA 94720, USA^b Keck Science Center, Claremont Colleges, Claremont, CA 91711, USA

Received 22 December 1998; received in revised form 11 March 1999; accepted 11 March 1999

Communicated by C.R. Doering

Abstract

Symmetry-increasing bifurcations of strange attractors in systems with $O(2)$ symmetry are shown to produce traveling waves that reverse their direction of propagation in a chaotic fashion. The resulting dynamics are illustrated using the normal form describing the triple zero instability. © 1999 Elsevier Science B.V. All rights reserved.

PACS: 05.45.-a; 47.20.Ky; 47.52.+j; 47.20.-k

Keywords: Waves; Symmetry-increasing bifurcations; Crises of strange attractors

In a previous Letter [1] we have identified a simple mechanism responsible for generating direction-reversing waves in systems with $O(2)$ symmetry. In translation-invariant systems on a line with periodic boundary conditions $O(2)$ symmetry is generated by translations $T_\ell: x \rightarrow x + \ell$ and the reflection $R: x \rightarrow -x$. Such systems often possess a *circle* of nontrivial steady states, parametrized by a phase ϕ representing the distance of a node from an arbitrarily chosen origin $x = 0$. Each of these states is reflection-symmetric and neutrally stable with respect to translations [2]. Direction-reversing waves (hereafter RW) result from a Hopf bifurcation from this circle of steady states that breaks their reflection symmetry [1]. The resulting RW are periodic in time (they reverse their direction of propagation in a periodic fashion), and if they are attracting produce a

reflection-symmetric *attractor*, even though at any instant the RW solution itself is *not* reflection-symmetric. In this Letter we describe a mechanism that produces RWs that reverse their direction of propagation *chaotically*. This mechanism involves symmetry-increasing bifurcations of (asymmetric) strange attractors [3,4] and is, like the above mechanism, of codimension one.

We illustrate the mechanism using the equations [1]

$$\frac{dz_1}{dt} = z_2, \quad (1)$$

$$\frac{dz_2}{dt} = z_3, \quad (2)$$

$$\frac{dz_3}{dt} = -\lambda z_1 - \nu z_2 - \eta z_3 + |z_1|^2 z_1. \quad (3)$$

These equations are the normal form for a triple zero

¹ Corresponding author. E-mail: knobloch@physics.berkeley.edu

bifurcation with $O(2)$ symmetry and as such have a number of applications, particularly in fluid dynamics [5]. Here z_1 is the complex amplitude of a physical field of interest, $\psi(x,t) = \text{Re}(z_1 e^{2\pi i x/L})$, where L is the spatial period of the system, and λ, ν , and η are real unfolding parameters: at $\lambda = \nu = \eta = 0$ the trivial state $(z_1, z_2, z_3) = (0,0,0)$ has three zero eigenvalues of double multiplicity. In the following we let $\phi = \arg(z_1)$. Thus, if $\phi > 0$ (< 0) $\psi(x,t)$ takes the form of a *wave* traveling to the left (right). For each $\phi \in [0, 2\pi)$ the system (1)–(3) has a reflection-invariant subspace $\Sigma_\phi = (z_1, z_2, z_3)$ with $\arg(z_j) = \phi$, $j = 1, 2, 3$; in these subspaces $\dot{\phi} = 0$. Different Σ_ϕ are related to each other by translation (rotation). Each contains the trivial steady state and may contain a pair of nontrivial steady states SS_ϕ and an oscillation in the form of either a symmetric or asymmetric periodic or chaotic standing wave (SW_ϕ), with asymmetric waves (ASW_ϕ) distinguished by their lack of reflection symmetry within Σ_ϕ with respect to the origin. Other solutions described below such as traveling waves (TW) and modulated waves (MW) do not lie in reflection-invariant subspaces.

Fig. 1 shows representative solutions to Eqs. (1)–(3) when $\nu = 2.0$, $\eta = 1.5$, projected onto the complex z_1 plane. At $\lambda = 5.0$ the SW_ϕ solutions shown in Fig. 1(a) are unstable to traveling wave disturbances and decay into stable TW. These TW have constant amplitude $|z_1|$ and constant nonzero $\dot{\phi}$ (Fig. 1(b)); because of reflection symmetry left- and right-propagating TW coexist. At $\lambda = 6.70$ there are two stable reflection-related tori, one with drift strictly to the left and the other strictly to the right. One of these tori is shown in Fig. 1(c), with Fig. 1(d) showing the corresponding time series for $\dot{\phi}$. If λ is increased to 7.37 each torus has period-doubled into chaos forming two reflection-related strange attractors, with $\dot{\phi}$ remaining bounded away from zero. One such attractor is shown in Fig. 1(e) with the corresponding time series in Fig. 1(f). At $\lambda = 7.39$ $\dot{\phi}$ is no longer bounded away from zero and changes sign irregularly, indicating chaotic reversals in the direction of propagation. As described below, these chaotic reversals are the result of a symmetry-increasing bifurcation of strange attractors associated with an (interior) crisis [6,7]. Fig. 2(a) shows one such reversal in the form of a space-time plot showing $\psi(x,t)$ for $\lambda = 7.39$ and $L = 100$. During this

reversal the drift in phase comes nearly to a complete halt and the oscillation temporarily resembles an asymmetric standing wave oscillating at constant ϕ . Fig. 2(b) shows that at other times the oscillation may temporarily resemble a standing wave *without* reversing direction, and that reversals may occur in which the oscillation does not resemble a standing wave for any appreciable time.

The behavior of Eqs. (1)–(3) is summarized in the bifurcation diagram shown in Fig. 3 with λ as the bifurcation parameter. For $\lambda < 0$ the trivial state is unstable, and as λ increases the trivial state acquires stability at a subcritical steady state bifurcation at $\lambda = 0$ and loses it again at a supercritical Hopf bifurcation at $\lambda = 3.000$. The Hopf bifurcation gives rise to a branch of stable TW and a branch of unstable periodic SW_ϕ . The TW lose stability to MW at $\lambda_{\text{MW}} \equiv 6.176$ which then undergo a torus-doubling cascade (hereafter type T torus-doubling cascade). Meanwhile each SW_ϕ undergoes a symmetry-breaking pitchfork bifurcation at $\lambda = 6.613$ giving rise to two asymmetric standing waves (ASW_ϕ) that are stable in each Σ_ϕ and have one real unstable Floquet multiplier perpendicular to Σ_ϕ until λ reaches $\lambda_{\text{PB}} \equiv 7.791$; here the period-doubled MW, having undergone a reverse period-doubling cascade (hereafter type PB torus-doubling cascade), terminates on the *circle* of ASW_ϕ in a parity-breaking bifurcation [8] and the ASW_ϕ acquire stability. As λ is increased further the ASW_ϕ branch terminates when the ASW_ϕ collide with a SS_ϕ fixed point forming a homoclinic orbit in Σ_ϕ . This occurs at $\lambda = 8.01$ and results in Shil'nikov dynamics in each Σ_ϕ , cf. [5]. The (reflection-symmetric) SW_ϕ branch terminates in a heteroclinic bifurcation, also associated with Shil'nikov dynamics, at $\lambda = 12.50$.

The evolution with λ of the strange attractors arising from the period-doubling cascades mentioned above is shown in Fig. 4. The figure shows the instantaneous value of $\dot{\phi}$ for a single attractor at each λ value whenever the trajectory pierces the Poincaré section defined by $\text{Re}(z_1 z_2) = 0$. At a given λ value the attractor may or may not be symmetric about $\dot{\phi} = 0$. In the latter case a reflection-related attractor is also present but is not shown. The reflection-symmetric attractors correspond to direction-reversing waves, and form as a result of symmetry-increasing or symmetry-decreasing bifurcations of

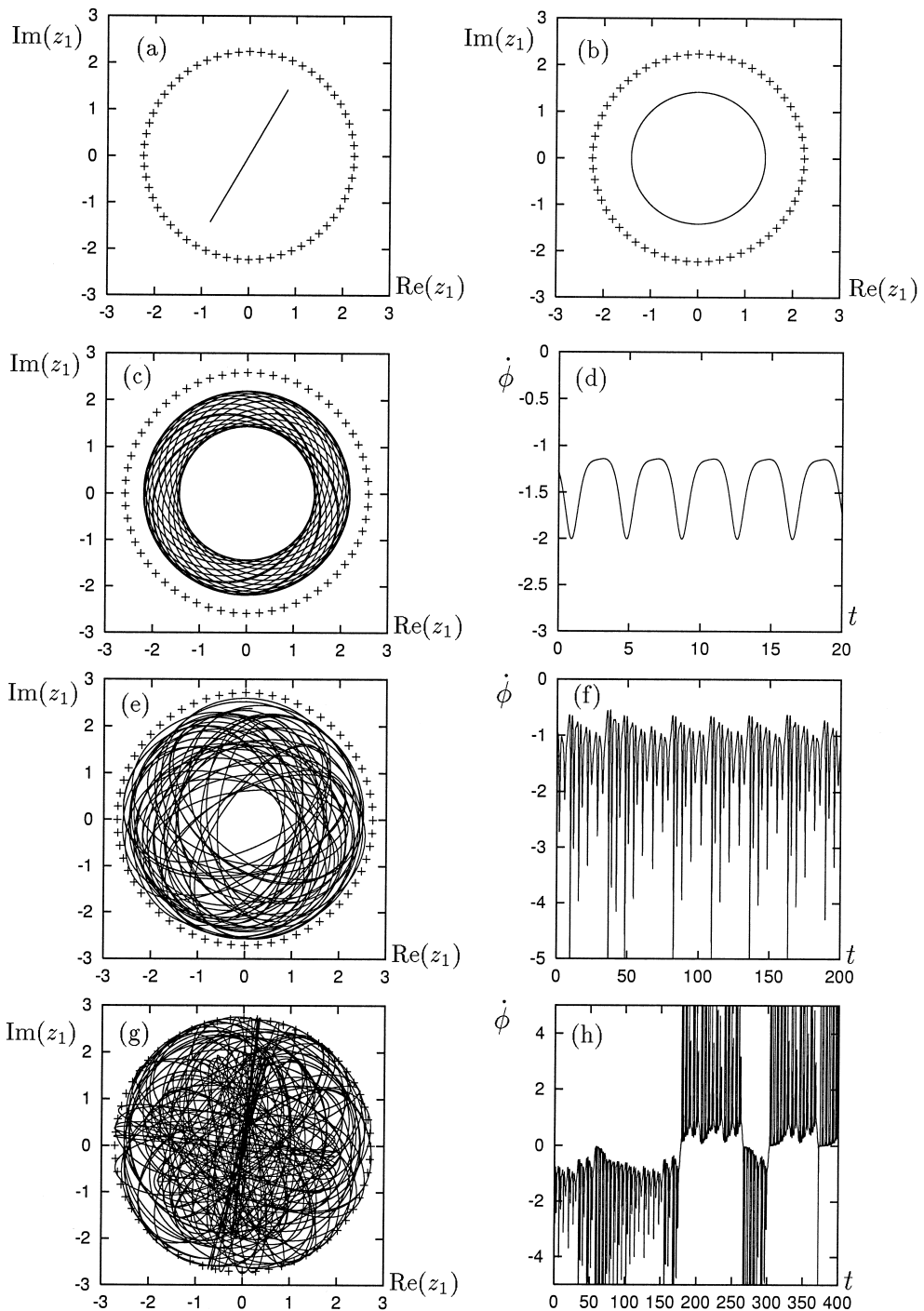


Fig. 1. Representative solutions to Eqs. (1)–(3) projected onto the complex z_1 plane; unstable SS_ϕ solutions are indicated by plus signs. (a) An unstable SW_ϕ solution and (b) a stable TW solution, both at $\lambda = 5.0$. (c,d) Stable MW solutions at $\lambda = 6.7$. (e,f) Stable chaotic solutions at $\lambda = 7.37$; since $\dot{\phi}$ is always of the same sign the waves always travel in the same direction. (g,h) Stable direction-reversing waves at $\lambda = 7.39$. The parameters are $\nu = 2.0$, $\eta = 1.5$.

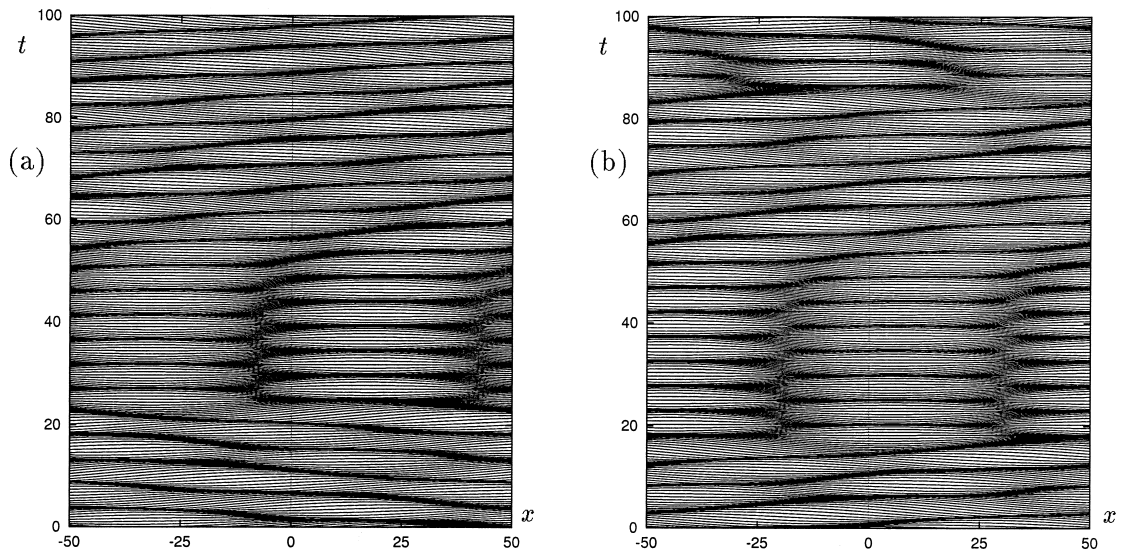


Fig. 2. Space-time representation of $\psi(x,t)$ at $\lambda = 7.39$ illustrating the physical manifestation of the reversals. Time increases upward.

strange attractors [3]. One such bifurcation occurs at $\lambda \approx 7.38$; at this λ value an (interior) crisis occurs in which an asymmetric strange attractor describing

chaotic waves with a preferred direction of propagation (cf. Fig. 1(e,f)) collides with an unstable (period-quadrupled) MW, producing a symmetric

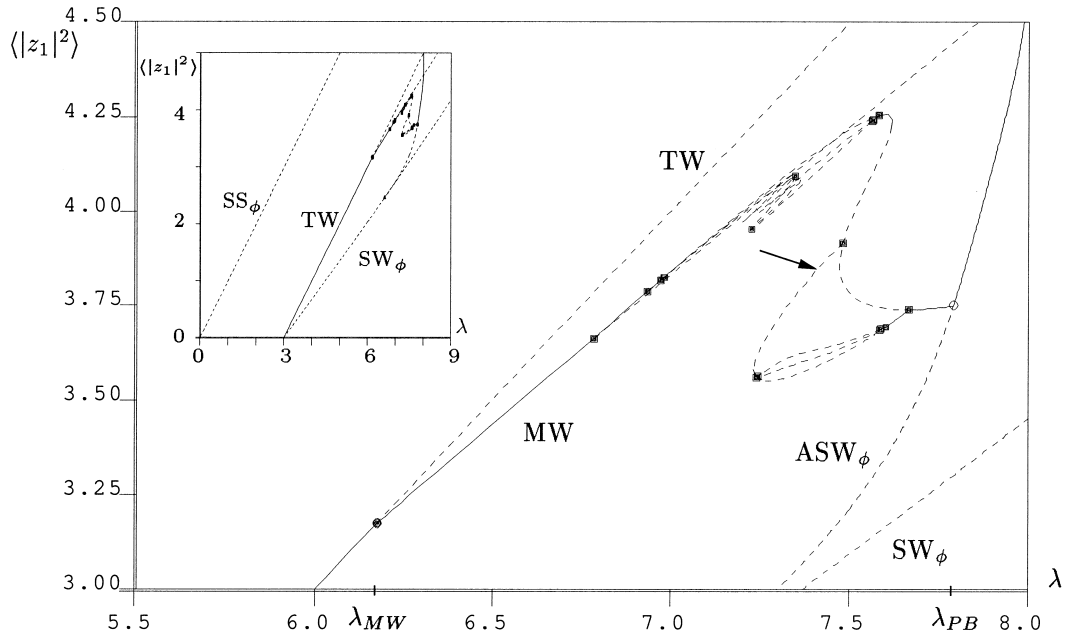


Fig. 3. Partial bifurcation diagram showing $\langle |z_1|^2 \rangle$, the time-average of $|z_1|^2$, as a function of λ for $\nu = 2.0$, $\eta = 1.5$. Solid (broken) lines indicate stable (unstable) branches. The parity-breaking bifurcation at λ_{PB} from the circle of asymmetric standing waves is indicated by the open circle; solid squares indicate period-doubling bifurcations. The arrow shows the unstable modulated wave involved in the interior crisis at $\lambda \approx 7.38$ as described in the text.

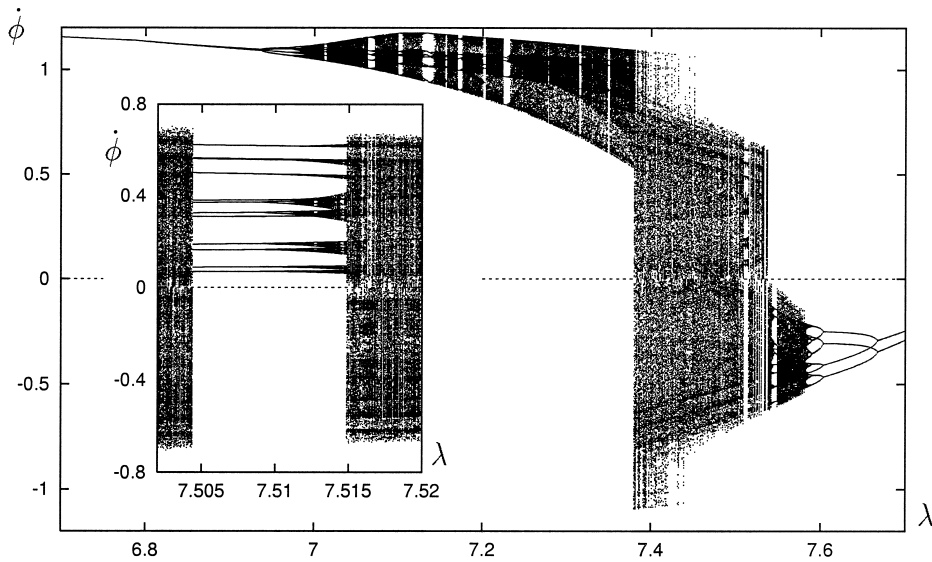


Fig. 4. Bifurcation diagram showing instantaneous values of $\dot{\phi}$ whenever the trajectory pierces the Poincaré section defined by $\text{Re}(z_1 z_2) = 0$ (from positive to negative values) after transients have died out. The diagram shows symmetry-increasing (-decreasing) bifurcations at which direction reversals first appear (disappear).

strange attractor and chaotic reversals (cf. Fig. 1(g,h)). In Ref. [4] such a symmetry-increasing bifurcation is called an attractor *explosion*. The explosion apparently occurs when the unstable manifold of the (asymmetric) standing waves ASW_ϕ becomes tangent to the stable manifold of the unstable MW indicated by the arrow in Fig. 3 and diamonds in Fig.

5 (cf. [9]). A different transition occurs as λ increases through 7.5045. At this value the symmetric strange attractor disappears and an asymmetric period 12 MW appears in a tangent bifurcation (see inset of Fig. 4). This orbit undergoes a period-doubling cascade as λ increases; at $\lambda = 7.515$ the resulting attractor undergoes an interior crisis once again

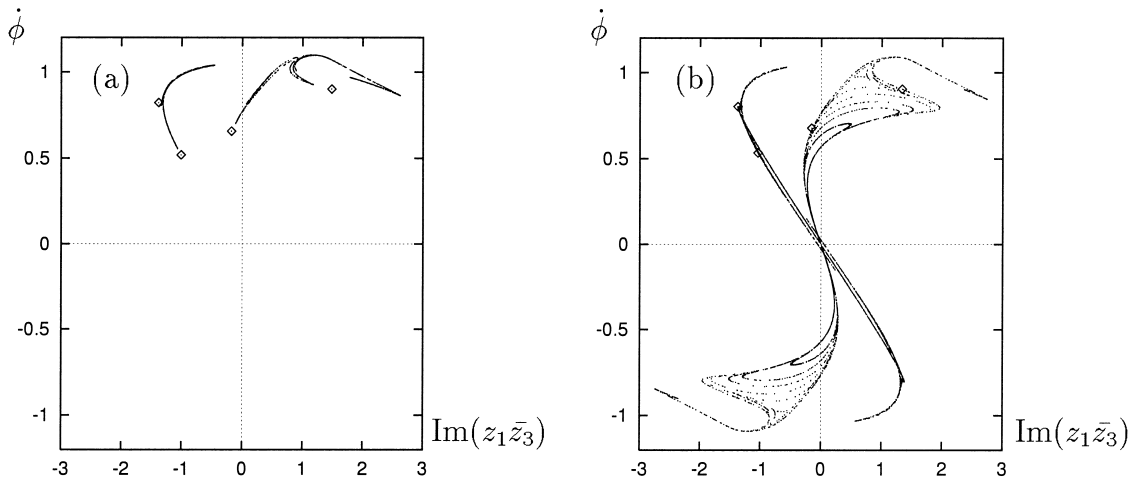


Fig. 5. The return map constructed as in Fig. 4 plotted against the two variables that are indicative of drift. (a) $\lambda = 7.37$, (b) $\lambda = 7.39$. The diamonds show the unstable modulated wave indicated by the arrow in Fig. 3. In this projection the Σ_ϕ subspaces all lie at the origin.

forming a reflection-symmetric strange attractor. There is also a symmetry-increasing bifurcation associated with a collision of strange attractors [4] as λ is *decreased* through 7.54. At this point a pair of symmetry-related strange attractors (only one of which is shown in Fig. 4) collide with the surface $\dot{\phi} = 0$. A different type of interior crisis occurs at $\lambda \approx 7.46$ at which the size of the reflection-symmetric attractor changes, but not its symmetry; more points would fill in the larger attractor present in the range $7.38 < \lambda < 7.46$.

We now discuss the two torus-doubling cascades in more detail, starting with the T cascade. Because of translation invariance one of the MW frequencies, ω_{TW} , can be removed by going into a traveling reference frame; in this frame the MW solutions are singly periodic with a period $T(\lambda)$. Near λ_{MW} the evolution of the spatial phase ϕ is therefore governed by the normal form

$$c_{n+1} = [1 + \alpha(\lambda - \lambda_{\text{MW}})]c_n + \beta c_n^2 + \dots, \quad (4)$$

where

$$c_n = \frac{\phi_n - \phi_{n-1}}{T/2^m} - \omega_{\text{TW}}, \quad \phi_n = \phi(nT/2^m).$$

Here ω_{TW} is the phase velocity of the TW solution from which the MW bifurcates, m is the number of period-doubling bifurcations which have occurred between λ_{MW} and λ , and α and β are constants. This map is the stroboscopic map with period $T/2^m$ with c_n the average phase velocity relative to the traveling wave over this time interval. (We strobe with period $T/2^m$ instead of T so that our strobe period is a continuous function of λ .) Thus the phase

dynamics near λ_{TW} are (locally) described by a *quadratic* map, with $c_n = 0$ corresponding to the TW state. On the other hand, near λ_{PB} , the corresponding map must be equivariant under reflections since the parity-breaking bifurcation generates both left- and right-propagating MW. Thus the normal form near λ_{PB} describing the evolution of the spatial phase is the *cubic* map, cf. [8],

$$c_{n+1} = [1 + \alpha(\lambda - \lambda_{\text{PB}})]c_n + \beta c_n^3 + \dots, \quad (5)$$

where the c_n are now defined by

$$c_n = \frac{\phi_n - \phi_{n-1}}{T/2^m}, \quad \phi_n = \phi(nT/2^m),$$

and $c_n = 0$ corresponds to the SW_b state. Despite their construction as normal forms the maps (4), (5) turn out to provide a good qualitative description of many features of the torus-doubling cascades. For example, period one fixed points of the maps satisfy

$$c = \left(-\frac{\alpha(\lambda - \lambda_B)}{\beta} \right)^\gamma, \quad (6)$$

where $\lambda_B = \lambda_{\text{MW}}, \gamma = 1$ for type T cascades and $\lambda_B = \lambda_{\text{PB}}, \gamma = \frac{1}{2}$ for type PB cascades. Fig. 6 compares values of c obtained by direct integration of Eqs. (1)–(3) near λ_{MW} and λ_{PB} with the corresponding fits to Eq. (6) shown as dashed lines. Of particular interest in the context of direction reversals is the fact that the cubic map (5) exhibits a pair of period-doubling cascades related by reflection (see e.g. [10]) which undergo a symmetry-increasing bifurcation when the reflection-related attractors collide at the origin [3]. This is analogous to the bifurcation responsible for the onset of chaotic reversals as λ

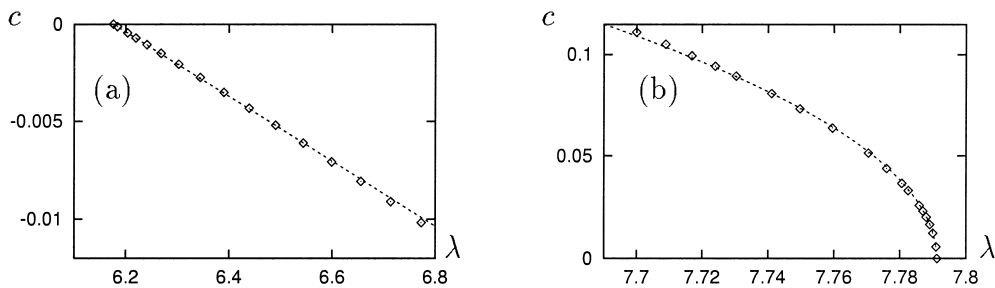


Fig. 6. Equilibrated values of $c \equiv \lim_{n \rightarrow \infty} c_n$ computed from Eqs. (1)–(3) as a function of λ near (a) λ_{MW} and (b) λ_{PB} (diamonds) compared with fits of the form Eq. (6) (dashed lines).

decreases from λ_{PB} . However, in order to obtain quantitative agreement between the map (5) and Eqs. (1)–(3) in this regime higher order terms in $(\lambda - \lambda_{\text{PB}})$ and c_n must be included; a similar statement holds for the map (4). Note that the maps (4) and (5) cannot describe the dynamics due to the interior crises found for Eqs. (1)–(3) since these involve MW not described by them.

The chaotic phase dynamics described here are a reflection of underlying amplitude chaos. More precisely, near λ_{PB} the phase velocity reflects the dynamics in the amplitude of the asymmetric part of the solution. However, the dynamics of the symmetric part of the solution may also be chaotic. When this is the case the map (5) must be augmented by a second map describing the dynamics in Σ_ϕ , as discussed by Lai [11]; direction reversals will still be produced by the collision of a pair of asymmetric attractors [11] but these can now exhibit strong on-off intermittency arbitrarily close to λ_{PB} .

In this Letter we have identified a new mechanism responsible for producing chaotically reversing waves. This mechanism is of codimension one and generates spontaneous reversals in systems with periodic boundary conditions, i.e., in systems in which sidewalls (and reflections from them) are absent. Such reflections are associated with reversals in the direction of propagation in other systems [12,13]. In the present system the onset of reversals is associated with a symmetry-increasing bifurcation of strange attractors which arise from cascades of torus-doubling bifurcations. The mechanism is a natural extension of the observation [14,15] that periodic RW can also be produced via a gluing bifurcation of asymmetric oscillations. Depending on the eigenvalues of the symmetric steady state involved, such a gluing bifurcation can itself produce chaotic dynamics and these can be of Lorenz or Shil'nikov type. In contrast, the mechanism described here does

not involve steady states at all. Other mechanisms generating chaotic reversals can be envisaged as well. These involve homoclinic connections of a circle of standing waves to itself, or heteroclinic connections between circles of steady states and standing waves (cf. [16,17]), and will be discussed elsewhere.

Acknowledgements

This work was supported in part by the National Science Foundation under Grant. No. DMS-9703684.

References

- [1] A.S. Landsberg, E. Knobloch, Phys. Lett. A 159 (1991) 17.
- [2] J.D. Crawford, E. Knobloch, Ann. Rev. Fluid Mech. 23 (1991) 341.
- [3] P. Chossat, M. Golubitsky, Physica D 32 (1988) 423.
- [4] M. Dellnitz, M. Golubitsky, I. Melbourne, Mechanisms of symmetry creation, in: Bifurcation and symmetry, eds. E. Allgower, K. Böhmer, M. Golubitsky, ISNM 104 (Birkhäuser, 1992), pp. 99–109.
- [5] A. Arméodo, P.H. Coullet, E.A. Spiegel, Geophys. Astrophys. Fluid Dyn. 31 (1985) 1.
- [6] C. Grebogi, E. Ott, J.A. Yorke, Phys. Rev. Lett. 48 (1982) 1507.
- [7] C. Grebogi, E. Ott, J.A. Yorke, Physica D 7 (1983) 181.
- [8] J.M. Greene, J.S. Kim, Physica D 33 (1988) 99.
- [9] C. Grebogi, E. Ott, F. Romeiras, J.A. Yorke, Phys. Rev. A 36 (1987) 5365.
- [10] J. Testa, G.A. Held, Phys. Rev. A 28 (1983) 3085.
- [11] Y.-C. Lai, Phys. Rev. E 53 (1996) R4267.
- [12] A.E. Deane, E. Knobloch, J. Toomre, Phys. Rev. A 37 (1988) 1817.
- [13] C. Martel, J.M. Vega, Nonlinearity 11 (1998) 105.
- [14] P.C. Matthews, M.R.E. Proctor, A.M. Rucklidge, N.O. Weiss, Phys. Lett. A 183 (1993) 69.
- [15] A.M. Rucklidge, P.C. Matthews, Nonlinearity 9 (1996) 311.
- [16] E. Knobloch, D.R. Moore, Phys. Rev. A 42 (1990) 4693.
- [17] E. Knobloch, D.R. Moore, European J. Mech. B 10, no. 2-Suppl. (1991) 37.